J|A|C|S
ARTICLES
Published on Web 09/08/2006

To Achieve Stable Spherical Clusters: General Principles and Experimental Confirmations

Zhongfang Chen,*,† Sven Neukermans,‡ Xin Wang,‡ Ewald Janssens,‡ Zhen Zhou,§ Roger E. Silverans,‡ R. Bruce King,† Paul von Ragué Schleyer,† and Peter Lievens*,‡

Contribution from the Department of Chemistry and Center for Computational Chemistry, University of Georgia, Athens, Georgia 30602, Laboratorium voor Vaste-Stoffysica en Magnetisme, Katholieke Universiteit Leuven, Celestijnenlaan 200D, B-3001 Leuven, Belgium, and Institute of New Energy Material Chemistry, Institute of Scientific Computing, Nankai University, Tianjin 300071, P. R. China

Received May 2, 2006; E-mail: chen@chem.uga.edu; peter.lievens@fys.kuleuven.ac.be

Abstract: General principles for designing stable highly symmetrical clusters are proposed. This approach takes advantage of both the extra stability of cage aromaticity and the good geometrical balance between the outer cage and the endohedral atom. The applicability of these design principles was confirmed by gas-phase experimental observations on group 14 element cages with endohedral Al's and also is illustrated by many literature examples of diverse systems.

Introduction

Highly symmetrical and chemically (quasi)inert clusters have long been sought because they may serve as ideal building blocks for tailored nanomaterials. Clusters with closed shells of electrons are good prospects. According to the cluster shell model, metal clusters containing the correct number of valence electrons, e.g., 2, 8, 20, 40, 58, ..., to close electronic shells should exhibit marked stability.[1] Wade's famous $2n + 2$ skeletal electron rule, typically applied to *closo* boranes and carboranes, predicts a different electron count[2] as does Hirsch's insightful $2(n + 1)^2$ electron counting rule, 2, 8, 18, 32, 50, ..., for spherical clusters[3] such as fullerenes[3a] and some well-known inorganic cages.[4] Various novel three-dimensional aromatic compounds have been designed according to such rules.[5] However, limitations arising from complications in the electronic structures of some clusters have been noted.[6] Close atomic packing is another important factor determining stability whereby clusters with 13, 55, 147, ... atoms would be magic.[7] Actually, both geometric and electronic considerations must be taken into account to achieve stable clusters, "it will be ideal if the close atomic packing as well as the electronic shell closures can be simultaneously achieved to give a cluster-enhanced stability."[8] Similar considerations have been pointed out since the early 1990s.[9] However, despite their physical and chemical basis, these two guidelines do not suffice. Although the recently generated $AlPb_{12}^+$, for example, has a close-packed icosahedral structure, the 50 valence electrons do not follow the cluster shell model and only correspond to the Hirsch rule superficially.[10] Some of the high angular momentum spherical molecular orbital levels are split and are not fully occupied. This results in nonoptimum electronic structures and a reduction or elimination of the aromaticity.

We now present general principles for the design of stable highly symmetrical clusters, which take advantage of both the extra stability of cage aromaticity[11] and good geometrical balance. Experimental confirmations are provided and literature examples are discussed.

Computational and Experimental Methods

Geometries were fully optimized and vibrational frequencies were computed to characterize the nature of the stationary points. Nucleus-

† University of Georgia.
‡ Katholieke Universiteit Leuven.
§ Nankai University.

(1) Knight, W. D.; Clemenger, K.; de Heer, W. A.; Saunders, W. A.; Chou, M. Y.; Cohen, M. L. *Phys. Rev. Lett.* **1984**, *52*, 2141. (b) de Heer, W. A. *Rev. Mod. Phys.* **1993**, *65*, 611.
(2) (a) Wade, K. *J. Chem. Soc. Chem. Commun.* **1971**, 792. (b) Wade, K. *Adv. Inorg. Chem. Radiochem.* **1976**, *18*, 1.
(3) (a) Hirsch, A.; Chen, Z.; Jiao, H. *Angew. Chem., Int. Ed.* **2000**, *39*, 3915. (b) Reiher, M.; Hirsch, A. *Chem. Eur. J.* **2003**, *9*, 5442. (c) For a recent review, see Chen, Z.; King, R. B. *Chem. Rev.* **2005**, *105*, 3613.
(4) Hirsch, A.; Chen, Z.; Jiao, H. *Angew. Chem., Int. Ed.* **2001**, *40*, 2834.
(5) (a) Chen, Z.; Jiao, H.; Hirsch, A.; Schleyer, P. v. R. *Angew. Chem., Int. Ed.* **2002**, *41*, 4309. (b) Chen, Z.; Hirsch, A.; Nagase, S.; Thiel, W.; Schleyer, P. v. R. *J. Am. Chem. Soc.* **2003**, *125*, 15507. (c) Johansson, M. P.; Sundholm, D.; Vaara, J. *Angew. Chem, Int. Ed.* **2004**, *43*, 2678.
(6) King, R. B.; Heine, T.; Corminboeuf, C.; Schleyer, P. v. R. *J. Am. Chem. Soc.*, **2004**, *126*, 430.
(7) Echt, O.; Sattler, K.; Recknagel, E. *Phys. Rev. Lett.* **1981**, *47*, 1121.
(8) Khanna, S. N.; Jena, P. *Phys. Rev. Lett.* **1992**, *69*, 1664.
(9) "The right fits both geometrically and electronically" strategy, pointed out by Schleyer and Boldyrev in 1991 (Schleyer, P. v. R.; Boldyrev, A. I. *J. Chem. Soc. Chem. Comm.* **1991**, 1536), has served to design rule-breaking molecules, such as those containing planar hypercooordinate carbon: (a) a typical example is D_{6h} CB_6^{2-} with a planar hexacoordinate carbon, see Exner, K.; Schleyer, P. v. R. *Science* **2000**, *290*, 1937. (b) See the most recent review Minkin, V. I.; Minyaev, R. M.; Hoffmann, R. *Russ. Chem. Rev.*, **2002**, *71*, 869.
(10) Neukermans, S.; Janssens, E.; Chen, Z.; Silverans, R. E.; Schleyer, P. v. R.; Lievens, P. *Phys. Rev. Lett.* **2004**, *92*, 163401.
(11) See reviews (a) Minkin, V. I.; Glukhovtsev, M. N.; Simkin, B. Y. *Aromaticity and Antiaromaticity*; John Wiley & Sons: New York, 1994. (b) Schleyer, P. v. R.; Jiao, H. *Pure Appl. Chem.* **1996**, *68*, 209. (c) Lloyd, D. *J. Chem. Inf. Comp. Sci.* **1996**, *36*, 442. (d) Krygowski, T. M.; Cyranski, M. K.; Czarnocki, Z.; Hafelinger, G.; Katritzky, A. R. *Tetrahedron* **2000**, *56*, 1783. (e) Schleyer, P. v. R. (guest editor) *Chem. Rev.* **2001**, special issue on Aromaticity (May). (f) Schleyer, P. v. R. (guest editor) *Chem. Rev.* **2005**, special issue on Delocalization-Sigma and Pi (October).

10.1021/ja062868g CCC: $33.50

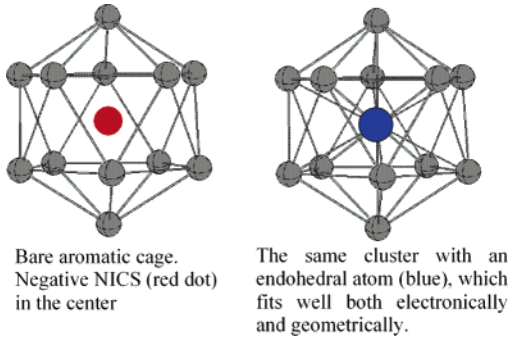

Figure 1. Procedure to design a stable spherical cluster.

independent chemical shifts (NICS, in ppm), a simple and efficient method to evaluate aromaticity,[12] were computed at the cage centers of the optimized geometries of the empty cage molecules using the gauge-independent atomic orbital (GIAO) method.[13] The LANL2DZdp ECP basis set was used for E_n^{2-}(E = Si, Ge, Sn, Pb; n = 5−12), whereas the LANL2DZ basis set was used for other species unless mentioned otherwise. The pseudopotential approximation has been demonstrated to be a reliable technique for NICS computations for heavy element clusters.[14] To gain further insight into the aromaticity and electronic structure of I_h E_{12}^{2-} and D_{4d} E_{10}^{2-} clusters, a recent refinement of the NICS method, CMO-NICS, was employed to compute the individual canonical molecular orbital contributions to the overall NICS value.[15]

Extensive potential energy surface scans have been performed for AlE_n^+ (E = Si, Ge, Sn, Pb; n = 5−12) (at B3LYP/6-31G* for E = Si, Ge; at B3LYP/LANL2DZ for E = Sn, Pb) to locate the most stable isomers for each composition. All the above computations employed the Gaussian 03 program.[16] In addition, $Th@Si_{20}$ systems were computed at the PBEPBE level[17] with the double numerical plus polarization (DNP) basis set[18a] using the DMol^3 program.[18]

Cationic Al doped group 14 element clusters AlE_n^+ (E = Si, Ge, Sn, Pb) were generated using a dual-target dual-laser vaporization source[19] and mass analyzed using reflectron time-of-flight mass spectrometry. Mass abundance spectra are shown in Figure 3. We reported the discovery and discussed reasons for the unusual stability of $AlPb_{12}^+$ and $AlPb_{10}^+$ (Figure 3d) recently.[10] The mass abundance spectrum for aluminum doped tin clusters (Figure 3c) features binary $AlSn_{1-16}^+$ clusters, among which $AlSn_6^+$, $AlSn_7^+$, $AlSn_{10}^+$, and $AlSn_{12}^+$ are especially prominent, particularly when compared to the corresponding pure Sn_n^+ clusters (peaks immediately before the $AlSn_n^+$ species). In contrast to the $AlPb_n^+$ clusters, $AlSn_{10}^+$ has the highest abundance in the tin set and $AlGe_n^+$ (n = 6, 7, and 10) among the germanium clusters (Figure 3b). The mass abundance spectrum for aluminum−silicon clusters is complicated to analyze due to additional signals from pure Si_n^+, pure Al_n^+, and multiply doped binary $Al_mSi_n^+$ species. In addition, the atomic masses of Al and Si differ by only one atomic mass unit (amu). However, as in the $AlGe_n^+$ set, $AlSi_n^+$ (n = 6 and 7) clusters are abundant, whereas $AlSi_{10}^+$ is much less pronounced (Figure 3a). Neither Figure 3a nor 3b provide any indication of special stability for $AlSi_{12}^+$ or $AlGe_{12}^+$, respectively.

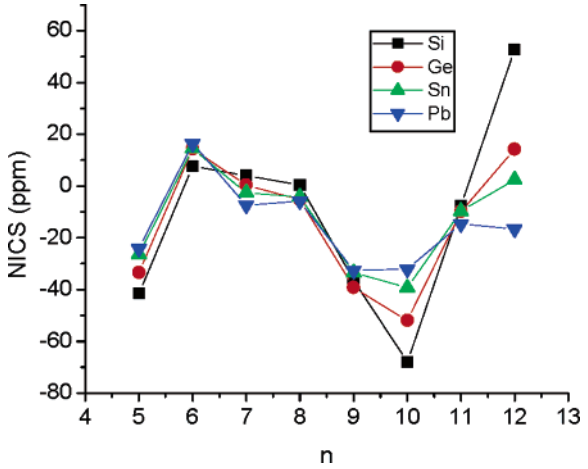

Figure 2. NICS values at the centers of E_n^{2-} cages computed at the GIAO-B3LYP/LANL2DZdp// B3LYP/LANL2DZdp level. Negative NICS values indicate diatropic (aromatic) structures, whereas positive values indicate paratropic (antiaromatic) species.

Results and Discussion

Procedures to Design Stable Spherical Clusters. Two main factors can be assumed to determine the stability of a spherical cluster, namely aromatic stabilization and close packing. Hence, the following procedure is proposed for molecular designs: a highly symmetrical hollow cage molecule, e.g., with icosahedral symmetry (Figure 1), is chosen initially. The number of electrons is then adjusted by the appropriate choice of atoms and charges to achieve significant aromatic character. The aromaticity can be assessed by computing the nucleus-independent chemical shifts (NICS)[12] at the hollow cage centers. Note that empty cage molecules, despite being aromatic, sometimes are not local minima in the symmetry imposed during the optimization. The second step of the procedure is to insert an endohedral guest atom (or atoms) of suitable size while maintaining the electron count of the empty cage by adjusting the overall charge. Electron transfer and a degree of covalent bonding between the endohedral atom and the outer cage can further enhance the binding energy. Providing that the guest atom is of the correct size, the endohedral complex should be a local minimum with no imaginary vibrational frequencies. This procedure is shown schematically in Figure 1.

Applications and Experimental Confirmations. Group 14 element cages E_n^{2-}. Previous NICS aromaticity computations on deltahedral Si_n^{2-} cages[6,20] have now been extended to systematic evaluations of the aromaticity of the group 14 deltahedral E_n^{2-} cages (E = Si, Ge, Sn, Pb, n = 5−12). Vibrational frequencies and NICS (Figure 2) were computed using the B3LYP/LANL2DZdp optimized geometries. Except that D_{2d} Si_8^{2-} distorts to D_2 symmetry, all the other empty deltahedral clusters are local minima (O_h Si_6^{2-} has two imaginary frequencies at B3LYP/LANL2DZdp, but is a local minimum at B3LYP/6-311+G*). Extensive searches of the

(12) (a) Schleyer, P. v. R.; Maerker, C.; Dransfeld, A.; Jiao, H.; Hommes, N. J. R. v. E. *J. Am. Chem. Soc.* **1996**, *118*, 6317. (b) For a recent review, see Chen, Z.; Wannere, C. S.; Corminboeuf, C.; Puchta, R.; Schleyer, P. v. R. *Chem. Rev.* **2005**, *105*, 3842.
(13) (a) Ditchfield, R. *Mol. Phys.* **1974**, *27*, 789. (b) Woliński, K.; Sadlej, A. J. *Mol. Phys.* **1980**, *41*, 1419. (c) Wolinski, K.; Hilton, J. F.; Pulay, P. *J. Am. Chem. Soc.* **1990**, *112*, 8251.
(14) Corminboeuf, C. *Chem. Phys. Lett.* **2006**, *418*, 437.
(15) (a) Heine, T.; Schleyer, P. v. R.; Corminboeuf, C.; Seifert, G.; Reviakine, R.; Weber, J. *J. Phys. Chem. A* **2003** , *107* , 6470. (b) Corminboeuf, C.; Heine, T.; Weber, J. *Phys. Chem. Chem. Phys.* **2003**, *5*, 246; Corminboeuf, C.; Heine, T.; Seifert, G.; Schleyer, P. v. R.; Weber, J. *Phys. Chem. Chem. Phys.* **2004**, *6*, 273.
(16) Frisch, M. J., et al. Gaussian 03, revision C.02; Gaussian, Inc.: Wallingford CT, 2004.
(17) Perdew, J. P.; Burke, K.; Ernzerhof, M. *Phys. Rev. Lett.* **1996**, *77*, 3865.
(18) (a) Delley, B. *J. Chem. Phys.* **1990**, *92*, 508. (b) Delley, B. *J. Chem. Phys.* **2000**, *113*, 7756.
(19) Bouwen, W.; Thoen, P.; Vanhoutte, F.; Bouckaert, S.; Despa, F.; Weidele, H.; Silverans, R. E.; Lievens, P. *Rev. Sci. Instr.* **2000**, *71*, 54.
(20) King, R. B.; Schleyer, P. v. R. In *Molecular Clusters of the Main Group Elements*; Driess, M., Nöth, H., Eds.; Wiley-VCH: Weinheim, Germany, 2003; pp 1−33.

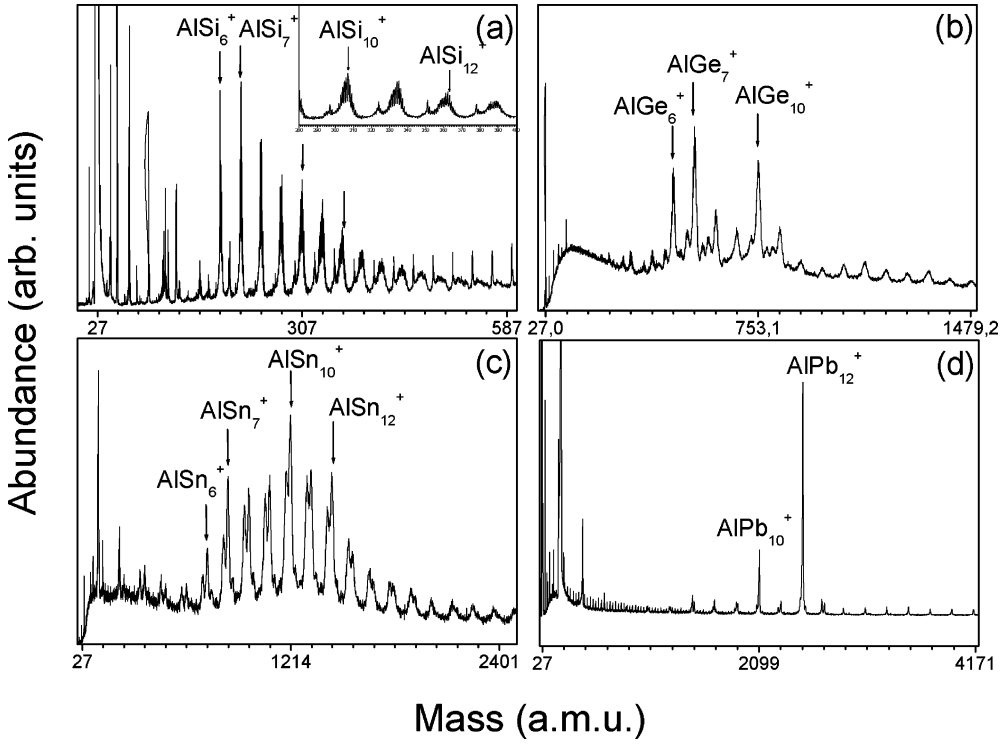

Figure 3. Mass abundance spectrum of mixed (a) $AlSi_n^+$, (b) $AlGe_n^+$, (c) $AlSn_n^+$, and (d) $AlPb_n^+$ clusters, showing the stability trend for AlE_{10}^+ and AlE_{12}^+. Among the AlE_{10}^+ species, $AlGe_{10}^+$, $AlSn_{10}^+$, and $AlPb_{10}^+$ are abundantly produced. Among the AlE_{12}^+ species, $AlSn_{12}^+$ and especially $AlPb_{12}^+$ are very prominent.

potential energy surface (PES) show that Si_6^{2-} and Ge_6^{2-}(O_h) are the global minima at B3LYP/6-311+G*, as are Sn_6^{2-} and Pb_6^{2-} (O_h) at the B3LYP/LANL2DZ level (see the Supporting Information for all of these results).

Several features in Figure 2 stand out. (1) Judging from their positive NICS values, all E_6^{2-} (O_h) species are moderately to highly antiaromatic. (2) All of the group 14 cages with the same number of vertices have similar NICS, but E_{10}^{2-} (**1**, D_{4d}) and E_{12}^{2-} (**2**, I_h) are notable exceptions. (3) The NICS values of E_{10}^{2-} (D_{4d}) clusters are all negative, but their magnitude decreases from silicon to lead. (4) The NICS trend for the E_{12}^{2-} (I_h) clusters was completely opposite to that for E_{10}^{2-} (D_{4d}), changing from highly antiaromatic (for silicon) to highly aromatic (lead).

The change from highly antiaromatic Si_{12}^{2-} $(I_h)^6$ to highly aromatic Pb_{12}^{2-} $(I_h)^{10}$ deserves explanation. CMO-NICS analysis (see the SI) shows that the paratropic contribution of the 5-fold degenerate h_g MO set (part of the incomplete 1 g^{10} shell)[21] dominates the total NICS of Si_{12}^{2-}. However, this major paratropic contribution diminishes down the group 14 elements (see the Supporting Information).

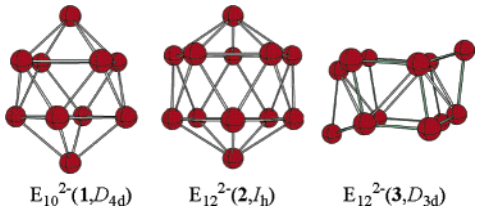

The significant difference in aromatic character along the $E_{12}^{2-}(I_h)$ series has direct consequences on their stabilities. Despite its compact geometric structure, I_h Si_{12}^{2-} is not the global minimum! A D_{3d} isomer (**3**) is 50.3 kcal/mol more stable at the B3LYP/LANL2DZdp level (37.5 kcal/mol at B3LYP/6-311+G*) than the I_h isomer. However, the I_h structures become gradually more favorable down the periodic table from Ge_{12}^{2-} to Pb_{12}^{2-} (see the Supporting Information). Very recently, the nonaromatic I_h Sn_{12}^{2-} (NICS 2.5 ppm) was detected in the form of $K^+[Sn_{12}]^{2-}$ in the gas phase; its stability may be attributed to the highly symmetrical close-packing.[22]

Also in 2006, Fässler, *et al.*[23] characterized the Pb_{10}^{2-} Zintl ion unambiguously in the solid state as the first empty 10-atom *closo* cluster of a group 14 element. It seems likely that other E_{10}^{2-} (E = Si, Ge, Sn) Zintl ions with even greater aromatic character will be isolated in the near future.

Pb_{12}^{2-} and all four E_{10}^{2-} clusters are highly aromatic and obey the first criterion for magic cluster construction, i.e., good electronic fit. In the second step, an Al^{3+} trication is inserted into the cavities of these aromatic cages. However, DFT computations show that among these five aromatic cages, only Pb_{12}^{2-}, Pb_{10}^{2-}, Sn_{10}^{2-}, and Ge_{10}^{2-} have suitable size cavities to host an Al^{3+} satisfactorily. The good geometrical fit between the host and the guest results in endohedral complexes, which are local minima. Si_{10}^{2-} is too small to accommodate Al^{3+} (NImag = 5). Because the E_{10}^{2-} and E_{12}^{2-} cages have high symmetries and compact structures ($AlSi_{10}^+$ is an exception,

(21) The g orbitals, which are nine-fold degenerate in the spherical K_h symmetry of atoms, split into a number of components in the actual lower point group symmetry in molecules. In icosahedral symmetry, the nine g orbitals split into four-fold and five-fold degenerate orbital sets. Only the latter is fully occupied (by five electron pairs) in an incomplete $1g^{10}$ shell. In the lower D_{4d} symmetry of the 10-vertex clusters, the corresponding five electron pairs occupy a non-degenerate orbital (the $1g^2$ part of an incomplete 1g shell) and two doubly degenerate orbital sets.

(22) Cui, L. F.; Huang, X.; Wang, L. M.; Zubarev, D. Y.; Boldyrev, A. I.; Li, J.; Wang, L. S. *J. Am. Chem. Soc.* **2006**, *128*, 8390.
(23) Spiekermann, A.; Hoffmann, S. D.; Fässler, T. F. *Angew. Chem., Int. Ed.* **2006**, *45*, 3459.

as the cage is too small), the stabilities are mainly governed by the aromaticity. Thus $AlGe_{10}^+$, $AlSn_{10}^+$, and $AlPb_{10}^+$ are expected to be highly stable. Unlike $AlSi_{12}^+$ and $AlGe_{12}^+$, $AlSn_{12}^+$ should be moderately stable and $AlPb_{12}^+$ should be highly stable (the stability of $AlSn_{12}^+$ is mainly due to its compact structure). Cages smaller than E_{10}^{2-} considered above are not large enough to accommodate an Al^{3+} cation inside and remain compact geometric structures; thus, they cannot be used to construct endohedral clusters, even though E_5^{2-} and E_9^{2-} are aromatic. The stability of the divalent-metal encapsulated I_h MSn_{12} clusters can be understood similarly.[24]

We have also computed the PESs very extensively for AlE_n^+ (E = Si, Ge, Sn, Pb) (details in the Supporting Information). We find that the D_{4d} AlE_{10}^+ (E = Ge, Sn, Pb) and the I_h $AlPb_{12}^+$, our proposed magic clusters, are lower in energy than all of the other isomers we surveyed and are the global minima. The Al atoms prefer exohedral or substitution sites in $AlSi_n^+$ (n = 5−12) and AlE_n^+(E = Ge, Sn, Pb; n = 5−9) (see the Supporting Information), owing to the lack of aromatic stabilization and (or) misbalance between the central dopant and the outer E_n^{2-} cage. The enhanced stability of our proposed magic clusters can also be seen from the computed binding energies (see the Supporting Information): D_{4d} AlE_{10}^+ (E = Ge, Sn, Pb) has significantly larger binding energy than the average value between AlE_9^+ and AlE_{11}^+; the binding energies from $AlPb_{11}^+$ to $AlPb_{12}^+$ increase rather sharply, indicating the unusually high stability of I_h $AlPb_{12}^+$.

Using our proposed principles, the most stable clusters can be obtained even without the tedious PES scan, although exceptions may exist due to the rather complex bonding of clusters. Note that a global minimum structure does not necessarily have the unusual stability associated with a "magic cluster" composition observed as a high abundance peak in a mass spectrometric experiment. This is illustrated by $AlGe_{12}^+$ and $AlSn_{12}^+$. Even though $AlGe_{12}^+$ (I_h) and $AlSn_{12}^+$ (I_h) are the lowest-energy minima among the many alternatives we computed, our experiment (see below) showed that neither of them is a magic cluster, owing to the moderate antiaromatic (for I_h Ge_{12}^{2-}) or nonaromatic (for I_h Sn_{12}^{2-}) character of the outer cages.

Although the mass distribution of clusters produced in a laser vaporization source does not necessarily reflect thermodynamic preference, under suitable source conditions, enhanced stabilities of certain cluster species nevertheless result in prominent abundances (e.g., the discovery of C_{60}). These stabilities are consistent with the experimental abundance of the AlE_{10}^+ (E = Ge, Sn, Pb) and AlE_{12}^+ (E = Sn, Pb) clusters (Figure 3). Note that AlE_{12}^+ (E = Si, Ge) clusters with antiaromatic outer E_{12}^{2-} cages have very small peak intensities. The gradual change of experimental abundances of AlE_{12}^+ (E = Si, Ge, Sn, Pb) species follows our predictions nicely.

Our experimental results clearly show that structural criteria alone are not adequate for judging the aromaticity of metal clusters. If structure were the major determinant of aromaticity, then *all* of the well packed I_h AlE_{12}^+ clusters would be highly aromatic and abundant experimentally. Although the E_6^{2-} (O_h) species are all moderately or highly paratropic (*anti*aromatic), they are located in deep valleys in the potential energy surface because there are no competing low-energy structural alternatives (see the Supporting Information). Therefore, the E_6^{2-} (O_h) set should be viable and provides promising synthetic targets for experimental characterization of genuinely antiaromatic metal-atom clusters.

The aromaticity/antiaromaticity trend of bare deltahedral group-14 clusters has direct consequences in the stability of their endohedral complexes. A strong correlation should exist between computed (anti)aromaticity and experimental abundance providing that the cavity is of suitable size (neither too large nor too small). For example, no stable divalent-metal-atom-doped $M@Si_{12}$ cluster with I_h symmetry has been reported experimentally. Although our computations show that endohedral Li^+, Be^{2+}, B^{3+}, Na^+, Mg^{2+}, and Al^{3+} are local minima inside I_h Si_{12}^{2-}, these I_h species are considerably higher in energy than open isomers with lower symmetry (see the Supporting Information). Moreover, although $Zn@Ge_{12}$ was predicted to be a magic cluster,[24a] our experiments showed no evidence for its enhanced stability.[25] This can be rationalized by the moderate antiaromaticity of Ge_{12}^{2-} (I_h) (NICS 14.2 ppm). All these observations emphasize that not only geometrical fit but also the aromatic vs antiaromatic character determines the stability of high-symmetry clusters.

Similarly, group 10 transition metals (Ni, Pd, and Pt) are favorable as endohedral atoms. DFT computations (Table 1) reveal the following minima, which can be expected to be magic clusters: $Ni@Ge_{10}^{2-}$, $Ni@Sn_{10}^{2-}$, $Ni@Pb_{10}^{2-}$, $Pd@Sn_{10}^{2-}$, $Pd@Pb_{10}^{2-}$, $Pt@Pb_{10}^{2-}$, $Ni@Pb_{12}^{2-}$, $Pd@Pb_{12}^{2-}$, and $Pt@Pb_{12}^{2-}$. There is no significant electron transfer between the d^{10} transition metals and the outer cages. These endohedral d^{10} atoms are exceptional among transition metals as they can be considered to be "pseudo-noble-gases," which neither donate nor accept cage electrons and interact only weakly with the surrounding polyhedron.[26] $M@Pb_{12}^{2-}$ (M=Ni, Pd, Pt)[27a,b] and $Ni@Pb_{10}^{2-}$ [27c] already have been isolated in the solid state by Eichhorn and co-workers and their structures have been characterized by X-ray diffraction.

CMO-NICS analysis revealed that the frontier a_1 molecular orbital (the 1 g^2 part of the incomplete 1 g shell)[21] has a highly paratropic contribution to the total NICS of E_{10}^{2-} cages (see the Supporting Information). Accordingly, removing two electrons from the HOMO of E_{10}^{2-} (D_{4d}) dianions results in more highly aromatic neutral clusters, even though they are all transition structures (NImag = 1). Incorporating suitable group 10 transition metals leads to the following local minima (Table 1), which are potential magic clusters: $Ni@Si_{10}$, $Ni@Ge_{10}$, $Pd@Ge_{10}$, $Pt@Ge_{10}$, $Pd@Sn_{10}$, $Pt@Sn_{10}$, and $Pt@Pb_{10}$. Guided by the experimental finding of 10 atom anionic clusters of group 14 elements doped with Co,[28] Kumar *et al.*[29] reported similar computational results earlier. Most recently, Han *et al.* found that $Ni@Ge_{10}$ is the most stable species of Ni-doped germanium

(24) (a) Kumar, V.; Kawazoe, Y. *Appl. Phys. Lett.* **2002**, *80*, 859. (b) Kumar, V.; Kawazoe, Y. *Appl. Phys. Lett.* **2003**, *83*, 2677.
(25) Neukermans, S.; Wang, X.; Veldeman, N.; Janssens, E.; Silverans, R. E.; Lievens, P. *Int. J. Mass. Spect.* **2006**, *252*, 145.
(26) King, R. B. *Dalton Trans.* **2004**, 3420.
(27) (a) Esenturk, E. N.; Fettinger, J.; Lam, Y. F.; Eichhorn, B. *Angew. Chem., Int. Ed.* **2004**, *43*, 2132. (b) Esenturk, E. N.; Fettinger, J.; Eichhorn, B. *J. Am. Chem. Soc.* **2006**, *128*, 9178. (c) Esenturk, E. N.; Fettinger, J.; Eichhorn, B. *Chem. Comm.* **2005**, 247.
(28) (a) Zhang, X.; Li, G.; Gao, Z. *Rapid Commun. Mass Spectrom.* **2001**, *15*, 1573. (b) Zhang, X.; Li, G.; Xing, X.; Zhao, X.; Tang, Z.; Gao, Z. *Rapid Commun. Mass Spectrom.* **2001**, *15*, 2399.
(29) Kumar, V.; Singh, A. K.; Kawazoe, Y. *Nano Lett.* **2004**, *4*, 677.

Table 1. NICS Values[a] at the Cage Center of Bare E_{10}^{2-}(D_{4d}), Pb_{12}^{2-}(I_h), and E_{10}(D_{4d}) Cages, the Number of Imaginary Frequencies, and the HOMO−LUMO Separation Energies[b] of Endohedral M@ E_{10}^{2-}, Pb_{12}^{2-}, and E_{10} Cages (at B3LYP/LANL2DZ)

	Si_{10}^{2-}		Ge_{10}^{2-}		Sn_{10}^{2-}		Pb_{10}^{2-}		Pb_{12}^{2-}	
NICS	−49.5		−39.2		−32.1		−24.8		−18.2	
M@	NImag	gap	NImag	gap	NImag	gap	NImag	gap	NImag	gap
Al^{3+}	5	2.28	0	2.49	0	2.35	0	2.63	0	3.09
Ni	2	2.06	0	2.21	0	2.16	0	2.29	0	2.66
Pd	5	1.67	2	1.92	0	1.96	0	2.12	0	2.75
Pt	5	1.40	4	1.73	1	1.81	0	1.97	0	2.68

	Si_{10}		Ge_{10}		Sn_{10}		Pb_{10}	
NICS	−71.7		−59.2		−49.9		−39.1	
M@	NImag	gap	NImag	gap	NImag	gap	NImag	gap
Ni	0	2.85	0	2.55	1	2.12	1	1.83
Pd	2	2.42	0	2.26	0	1.98	1	1.75
Pt	2	2.55	0	2.38	0	2.10	0	1.86

[a] ppm, at GIAO-B3LYP/LANL2DZ// B3LYP/LANL2DZ. [b] Gap, in eV.

clusters $NiGe_n$ ($n = 1-13$) according to the computed averaged binding energies.[30]

Our principle can explain the high stability of some metal-encapsulated silicon and germanium clusters very well.[31] For example, Si_{16}^{4-}, with either the fullerene-like (**4**) or the Frank-Kasper polyhedral (**5**) structure, is aromatic (NICS values are −40.9 and −22.9 ppm, respectively). But neither structure is a local minimum (NImag = 7 and 3, respectively). Adding an endohedral metal atom with four valence electrons, such as Ti and Zr, results in the stable clusters predicted by Kumar *et al.*[32] The MSi_{16} (M=Ti, Sc^-, and V^+) magic clusters were characterized experimentally in the gas phase.[33] Most recently, $[Pd_2@Ge_{18}]^{4-}$ (**6**), the largest single-cage deltahedral cluster comprised of a Ge_{18} cage and two central palladium atoms, was isolated by Goicoechea and Sevov.[34] Its high stability can also be rationalized by our principle: the empty Ge_{18}^{4-}(D_{3d}) cage is highly aromatic (NICS −43.5 ppm at the cage center), the two d^{10} endohedral palladium atoms result in a compact cluster. Note that the two palladium atoms are separated by 2.831 Å. This distance is longer than the internuclear separation (2.751 Å) in palladium metal.[35] Hence, the two palladium atoms may be separated inside the cage, and $2Pd@Ge_{18}^{4-}$ may be a better description for this cluster. Additional endohedral Zintl ions can be expected by taking advantage of the aromaticity of the bare Zintl ion cages.[36]

In cases where good geometric balance between the encapsulated atom and the outer cage is lacking, only distorted clusters can be expected. Very recently, Th@Si_{20} (**7**, I_h) was proposed by Kumar *et al.*[37] as a stable cluster. The stability of I_h M@Si_{20} (M = tetravalent metal) can be rationalized by assuming the transfer of four electrons from the central thorium atom to the outer Si_{20} cage, which might result in extra stabilization due to the highly aromatic silicon cage (NICS −88.3 ppm for I_h Si_{20}^{4-}). Despite this possibility and the relatively compact structure, I_h Th@Si_{20} is *not* a local minimum; a C_{2h} minimum is 4.5 kcal/mol lower in energy at PBEPBE/DNP level.[38] Smaller endohedral atoms such as Ti, Zr and Hf also are not large enough to stabilize the Si_{20}^{4-}(I_h) cage (NImag = 4 for all the three species, see the Supporting Information). The distorted structure of Zr@Si_{20} was found earlier.[39]

On the other hand, an aromatic outer cage is equally important to achieve highly stable spherical clusters. Recently, Zeng *et al.*[40] found that the tetrahedral fullerene Si_{28} cage can be stabilized when it encapsulates a tetrahedral metallic cluster (Al_4 or Ga_4). However, by itself, the outer Si_{28}^{4-} cage is nonaromatic (NICS −1.8 ppm at GIAO-BP86/6-31G*//BP86/6-31G*). This indicates that the stabilities of these $M_4@Si_{28}$ clusters mainly comes from the close-packing and the aromaticity of the encapsulated M_4 cluster. Endohedral silicon fullerenes with greater stability can be expected if the outer silicon cages are aromatic.

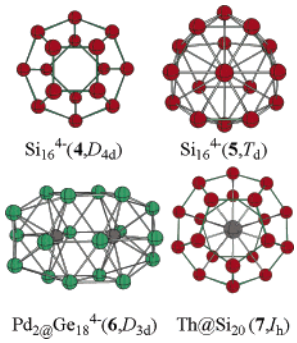

Gold Clusters. Gold shows unusual physicochemical properties owing to relativistic effects.[41] Various electron counting rules have been proposed to rationalize the stability of gold

(30) Wang, J.; Han, J. *J. Phys. Chem. B* **2006**, *110*, 7820.
(31) For a review, see Kumar, V. *Bull. Mater. Sci.* **2003**, *26*, 109.
(32) (a) Kumar, V.; Kawazoe, Y. *Phys. Rev. Lett.* **2001**, *87*, 045503; *Phys. Rev. Lett.* **2003**, *91*, 199901 (Erratum). (b) Kumar, V.; Briere, T. M.; Kazazoe, Y. *Phys. Rev. B.: Condens. Matter Mater. Phys.* **2003**, *68*, 155412. (c) Kumar, V.; Majumder, C.; Kawazoe, Y. *Chem. Phys. Lett.* **2002**, *363*, 319. (d) Lu, J.; Nagase, S. *Phys. Rev. Lett.* **2003**, *90*, 115506.
(33) Koyasu, K.; Akutsu, M.; Mitsui, M.; Nakajima, A. *J. Am. Chem. Soc.* **2005**, *127*, 4998.
(34) Goicoechea, J. M.; Sevov, S. *J. Am. Chem. Soc.* **2005**, *127*, 7676.
(35) Sutton, L. E., Ed. In *Table of interatomic distances and configuration in molecules and ions*, Supplement 1956−1959, Special publication No. 18; Chemical Society: London, UK, 1965.
(36) (a) Fässler, T. F.; Hoffmann, D. *Angew. Chem., Int. Ed.* **2004**, *43*, 6242. (b) Janssens, E.; Neukermans, S.; Lievens, P. *Curr. Opin. Solid State Mater. Sci.* **2004**, *8*, 185.
(37) Singh, A. K.; Kumar, V.; Kawazoe, Y. *Phys. Rev. B: Condens. Matter Mater. Phys.* **2005**, *71*, 115429.
(38) NImag = 12 at the B3LYP and PW91PW91 levels with ECP basis sets (Stuttgart RSC 1997 ECP basis set for Th, LanL2DZ basis set for Si); NImag = 4 at PBEPBE/DNP. At the last level, mode following of the first imaginary frequency led to the C_{2h} mimimum, which has one negligibly-small imaginary frequency ($25cm^{-1}$).
(39) Sun, Q.; Wang, Q.; Briere, T. M.; Kumar, V.; Kawazoe, Y.; Jena, P. *Phys. Rev. B:* **2002**, *65*, 235417.
(40) Gao, Y.; Zeng, X. C. *J. Chem. Phys.* **2005**, *123*, 204325.

Table 2. Number of Imaginary Frequencies, NICS Values (ppm) at the Cage Centers of the Empty Gold Clusters, and Spherical Clusters Predicted to Be Stable Using the Principles Proposed in This Paper[a]

				true minima	
	symmetry	NImag	NICS	experimentally known	awaiting verification
Au_6^{2-}	O_h	0	−38.1	$[C@Au_6]^{2+}$,[42] [b]	Au_6^{2-} [c]
Au_8	T_d	0	−30.8		Au_8 [d]
Au_{10}^{2+}	D_{4d}	0	−36.6	Au_{10}^{2+}, $[Au@Au_{10}]^{3+}$,[43] [e]	
Au_{12}^{4+}	I_h	3	−34.2	$[Pd@Au_{12}]^{4+}$,[44] $[Au@Au_{12}]^{5+}$,[45]	$[Ni@Au_{12}]^{4+}$, $[Pt@Au_{12}]^{4+}$
Au_{12}^{6-}	I_h	5	−54.3	$Mo@Au_{12}$, $W@Au_{12}$ [46]	
Au_{14}^{4-}	D_{2d}	0	−53.0		$M@Au_{14}$(M=Zr,Hf), $M@Au_{14}^-$(M=Sc,Y) [47]
Au_{32}	I_h	0	−100		Au_{32},[5c] $Ni_6@Au_{32}$ [48]

[a] Geometry and frequency computations were performed at the B3LYP/LANL2DZ level; NICS values were computed at GIAO-B3LYP/LANL2DZ on the optimized structures. [b] $[C@Au_6]^{2+}$ has three imaginary frequencies, but the largest is only 11.3i cm^{-1}. [c] $Au_6^{2-}(O_h)$ is ca. 30 kcal/mol more stable than the planar D_{3h} and C_{2v} isomers at the MP2/LANL2DZ level (see the Supporting Information). [d] $Au_8(T_d)$ is the most stable isomer at MP2 and CCSD(T) levels, see ref 49. [e] $[Au@Au_{10}]^{3+}$ has two small imaginary frequencies, but the larger is only 18i cm^{-1}.

clusters,[41b] which have been studied extensively recently.[41] Table 2 summarizes the stable clusters designed using our principles. All of the empty gold cages are aromatic, as indicated by their highly negative (diatropic) NICS values. A stable spherical cluster is expected to result, provided that there is a good match, geometrically and electronically, between the cage and an enclosed atom. For example, C^{4+} fits into the Au_6^{2-} (O_h) cage cavity well. Consequently, the spherical cluster $[C@Au_6]^{2+}$ (or $C^{4+}@Au_6^{2-}$) is a stable local minimum; however, the isoelectron B^{3+} and N^{5+} species do not have the correct size for effective inclusion and their endohedral complexes have three and six imaginary frequencies, respectively.

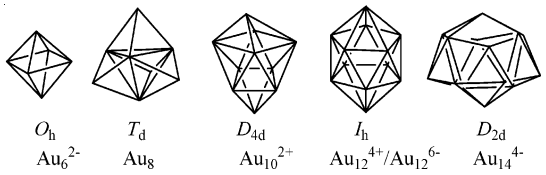

Very recently, it was found that the free-standing gold cluster anions Au_n^- ($n = 16-18$) are hollow golden cages,[50] it is highly possible that golden cages of such sizes (ca. 6 Å) can accommodate a guest atom (or guest atoms) inside to form stable spherical clusters, as pointed out by the original authors.

Conclusion

In summary, general principles based both on three-dimensional aromatic stabilization and on close-packing structures can be employed to design various stable high-symmetry clusters. The applicability of these principles has been confirmed by our experiments and supporting computations on group 14 element cages with endohedral Al's and is further illustrated by many literature reports of cages with endohedral d^{10} transition metal atoms, which do not affect the skeletal bonding or the skeletal electron count. All these examples show that NICS can serve not only as a measure of aromaticity but also can help to design stable clusters. These general principles explain the stability of various endohedral cluster compounds. Further applications, to endofullerenes,[51] for example, are underway.

Acknowledgment. This work was supported by the National Science Foundation Grant CHE-0209857 in Georgia, by the Fund for Scientific Research - Flanders (Belgium) (FWO), the Flemish Concerted Action Research Program (GOA), the Belgian Interuniversity Poles of Attraction Program (IAP) in Leuven, and by NSFC (50502021) in China. S.N. and E.J. thank the FWO for financial support. We thank the referees for critical comments and helpful suggestions. We also thank the Research Computing Center of the University of Georgia for providing computational resources.

Note added in proof. After we submitted this manuscript, Chen *et al.*[52] reported their theoretical studies on the electronic structures and stabilities of cationic MPb_{12}^+ clusters (M = B, Al, Ga, In, and Tl), and presented the MO-NICS analysis of I_h Pb_{12}^{2-}. After the acceptance of this manuscript, Wang *et al.*[53] reported the gas-phase production and characterization of Pb_{12}^{2-} in the form of $K^+[Pb_{12}]^{2-}$.

Supporting Information Available: NICS values at cage centers of E_n^{2-} (E = Si, Ge, Sn, Pb; $n = 2-12$), energy data of D_{3d} and I_h isomers of E_{12}^{2-} and their endohedral compounds, optimized structures and energy data of E_6^{2-}, AlE_n^+ ($n = 5-12$, E = Si, Ge, Sn, Pb) and Au_6^{2-} isomers, the summary of the most stable isomers of AlE_n^+ ($n = 5-12$, E = Si, Ge, Sn, Pb), the computed binding energies and the second difference in binding energies of the most stable isomers of AlE_n+, CMO-NICS analysis of I_h E_{12}^{2-} and D_{4d} E_{10}^{2-} (E = Si, Ge, Sn, Pb) clusters, the full citation of ref 16, as well as the Gaussian archive files of the optimized structures. This material is available free of charge via the Internet at http://pubs.acs.org.

JA062868G

(41) See recent reviews, (a) Schwerdtfeger, P. *Angew. Chem., Int. Ed*. **2003**, *42*, 1892. (b) Pyykkö, P. *Angew. Chem., Int. Ed.* **2004**, *43*, 4412. (c) Neukermans, S.; Janssens, E.; Tanaka, H.; Silverans, R. E.; Lievens, P. *Phys. Rev. Lett.* **2003**, *90*, 033401.
(42) Scherbaum, F.; Grohmann, A.; Huber, B.; Krüger, C.; Schmidbaur, H. A*ngew. Chem., Int. Ed. Engl.* **1988**, *27*, 1542.
(43) Copley, R. C. B.; Mingos, D. M. P. *J. Chem. Soc. Dalton Trans.* **1996**, 479.
(44) Laupp, M.; Strähle, J. *Angew. Chem., Int. Ed. Engl*. **1994**, *33*, 207.
(45) Briant, C. E.; Theobald, B. R. C.; White, J. W.; Bell, L. K.; Mingos, D. M. P. *J. Chem. Soc. Chem. Commun.* **1981**, 201.
(46) (a) Li, X.; Kiran, B.; Li, J.; Zhai, H. J.; Wang, L. S. *Angew. Chem., Int. Ed.* **2002**, *41*, 4786. (b) Predicted by Pyykkö, P.; Runeberg, N. *Angew. Chem., Int. Ed.* **2002**, *41*, 2174.
(47) Gao, Y.; Bulusu, S.; Zeng, X. C. *J. Am. Chem. Soc.* **2005**, *127*, 15680.
(48) Kruger, S.; Stener, M.; Rosch, N. *J. Chem. Phys.* **2001**, *114*, 5207.
(49) Olson, R. M.; Varganov, S.; Gordon, M. S.; Metiu, H.; Chretien, S.; Piecuch, P.; Kowalski, K.; Kucharski, S. A.; Musial, M. *J. Am. Chem. Soc.* **2005**, *127*, 1049.
(50) Bulusu, S.; Li, X.; Wang, L. S.; Zeng, X. C. *Proc. Nat. Acad. Sci.* **2006**, *103*, 8326.
(51) For recent reviews, see (a) Guha, S.; Nakamoto, K. *Coord. Chem. Rev.* **2005**, *249*, 1111. (b) *Endofullerenes, A New Family of Carbon Clusters*; Akasaka, T., Nagase, S., Eds.; Kluwer Academic Publishers: Norwell, MA, 2002. (c) Shinohara, N. *Rep. Prog. Phys.* **2000**, *63*, 843.
(52) Chen, D. L.; Tian, W. Q.; Lu, W. C.; Sun, C. C. *J. Chem. Phys.* **2006**, *124*, 154313.
(53) Cui, L. F.; Huang, X.; Wang, L. M.; Li, J.; Wang, L. S. *J. Phys. Chem. A* **2006**, *110*, 10169.